Inverse Problems in Space Physics

Bernd Inhester, May 2002

The program

Part I: Examples
- Image deblurring
- Tomography
- Radiative transfer inversion
- Helioseismology

Part II: Mainly direct methods
- Fourier transforms
- Singular value decomposition
- Backus-Gilbert or Mollifier method

Part III: Mainly Iterative methods
- Noise and a priori knowledge
- Iteration algorithms
- Regularization by Tikhonov
- Nonlinear problems
- Gencode and Neural networks

Literature

Introductions to Inverse Problems

I.J.D. Craig and J.C. Brown, Inverse Problems in Astronomy, Adam Hilger Ltd. Bristol, 1986. (An introduction, we dont have it in our library, but I have a copy)

J.A. Scales and M.L. Smith, Introductory Geophysical Inverse Theory, Samizdat Press, 1997. (freely available in internet: `http://samizdat.mines.edu`)

More comprehensive treatments are

A. Tarantola, Inverse Problems, Elsevier, 1987. (In the library at [G6 81], a bit old-fashioned)

R. Parker, Geophysical Inverse Theory, Princeton, 1994. (Standard reference for gephysicists, often quoted, should perhaps be bought by the library)

A first aid for practical problem solving is good old

W.H. Press, B. Flannery, S.A. Teukolsky, W.T. Vetterling, Numerical Recipies, Cambridge University Press, 1986. (The library code is [G6 70]. There are heavily revised more recent editions, the latest version is available in the internet:
`www.ulib.org/webRoot/Books/Numerical_Recipies`

Image deblurring: The phase function

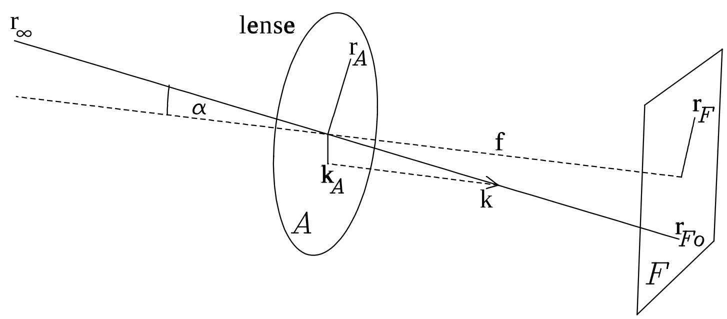

Geometry for the calculation of the point spread function, $\mathcal{A}$ is the plane of the aperture with a lense in front, $\mathcal{F}$ is the focal plane at a distance f from the aperture. An object is assumed infinitly away in direction of $\boldsymbol{r}_\infty$ and has its geometrical image at $\boldsymbol{r}_{Fo}$ in the focal plane.

Electrical wave field in focal plane F from a point source at $\boldsymbol{r}_\infty$ is

$$\boldsymbol{E}(\boldsymbol{r}_F, t) = \boldsymbol{E}_0 \frac{k\mathrm{e}^{-i\omega t}}{i2\pi f} \int_A \mathrm{e}^{i\Phi(\boldsymbol{r}_F, \boldsymbol{r}_A)}\, d^2(\boldsymbol{r}_A)$$

There are three contributions to the final phase of the field on the focal plane

$$\Phi(\boldsymbol{r}_F, \boldsymbol{r}_A) = \underbrace{\boldsymbol{k}_A \cdot \boldsymbol{r}_A}_{\text{init phase in front of lense}} + \underbrace{\Delta\phi_{\text{lense}}(r_A)}_{\text{phase change due to lense}} + \underbrace{k|\boldsymbol{r}_F + \boldsymbol{f} - \boldsymbol{r}_A|}_{\text{phase change due to propagation from plane } \mathcal{A} \text{ to plane } \mathcal{F}}$$

Making rigorous use of the Fraunhofer approximation

$$f \gg r_A \gg r_F$$

and
$$\Delta\phi_{\text{lense}} \equiv \phi_0 - \sqrt{f^2 + r_A^2}\,, \quad \boldsymbol{r}_{Fo} \equiv \frac{f}{k}\boldsymbol{k}_A$$

gives
$$\Phi(\boldsymbol{r}_F, \boldsymbol{r}_A) = \phi_0 - \frac{k}{f}(\boldsymbol{r}_F - \boldsymbol{r}_{Fo}) \cdot \boldsymbol{r}_A$$

Image deblurring: The point spread function

For a circular aperture area A with radius R we have

$$\int_A \mathrm{e}^{i\Phi(\boldsymbol{r}_F, \boldsymbol{r}_A)}\, d^2(\boldsymbol{r}_A) = \mathrm{e}^{i\phi_0} \int_A \mathrm{e}^{-i\frac{k}{f}(\boldsymbol{r}_F - \boldsymbol{r}_{Fo}) \cdot \boldsymbol{r}_A}\, d^2(\boldsymbol{r}_A)$$
$$= 2\pi R^2 \frac{\mathrm{J}_1(\frac{kR}{f}|\boldsymbol{r}_F - \boldsymbol{r}_{Fo}|)}{\frac{kR}{f}|\boldsymbol{r}_F - \boldsymbol{r}_{Fo}|} \mathrm{e}^{i\phi_0}$$

which is essentially the 2D Fourier transform of the aperture area A where the wave number is $|\boldsymbol{r}_F - \boldsymbol{r}_{Fo}|/f$ times the wave number k of the electromagnetic wave

$\longrightarrow$ final field is

$$\boldsymbol{E}(\boldsymbol{r}_F, t) = \boldsymbol{E}_0 \frac{kR^2}{f} \frac{\mathrm{J}_1(\frac{kR}{f}|\boldsymbol{r}_F - \boldsymbol{r}_{Fo}|)}{\frac{kR}{f}|\boldsymbol{r}_F - \boldsymbol{r}_{Fo}|} \mathrm{e}^{i(\phi_0 - \frac{\pi}{2} - \omega t)}$$

$\longrightarrow$ intensity in the focal plane

$$I(\boldsymbol{r}_F) = \frac{c}{2}|\boldsymbol{E}(\boldsymbol{r}_F, t)|^2 =$$
$$\underbrace{\pi R^2 \frac{c}{2}\boldsymbol{E}_0^2}_{P_0} \frac{1}{\pi} \left(\frac{kR}{f}\right)^2 \left(\frac{\mathrm{J}_1(\frac{kR}{f}|\boldsymbol{r}_F - \boldsymbol{r}_{Fo}|)}{\frac{kR}{f}|\boldsymbol{r}_F - \boldsymbol{r}_{Fo}|}\right)^2$$

P_0 (power collected in aperture area)

If instead of a discrete point source ideally focussed at $\boldsymbol{r}_{Fo}$, we have a distributed source of brightness, we finally have to replace

$$P_0 \longrightarrow I_0(\boldsymbol{r}_{Fo}) d^2\boldsymbol{r}_{Fo}$$

Image deblurring: The inverse problem

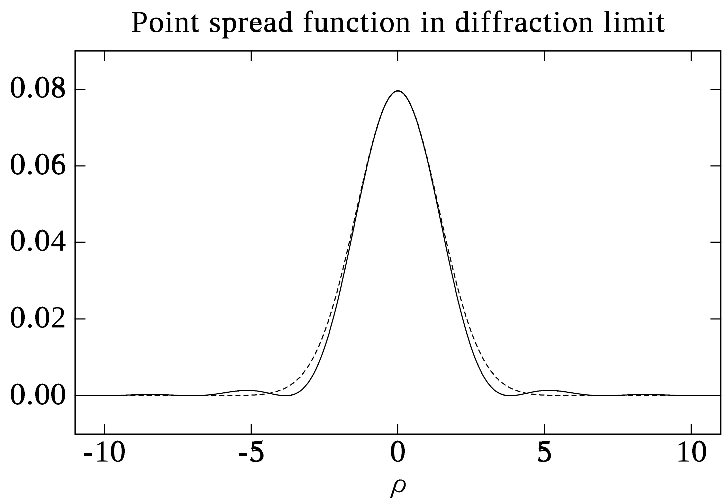

Cross section through the point spread function $(1/\pi)(J_1(\rho)/\rho)^2$ *and a Gaussian* $(1/4\pi)\exp-(\rho/2)^2$ *of similar shape (dashed).*

The final expression is

$$\underbrace{I(\boldsymbol{r}_F)}_{\text{Data}} = \int_F \underbrace{\frac{1}{\pi}\left(\frac{kR}{f}\right)^2 \left(\frac{\mathrm{J}_1(\frac{kR}{f}|\boldsymbol{r}_F - \boldsymbol{r}_{Fo}|)}{\frac{kR}{f}|\boldsymbol{r}_F - \boldsymbol{r}_{Fo}|}\right)^2}_{\text{Kernel}} \underbrace{I_0(\boldsymbol{r}_{Fo})}_{\text{Model}}\, d^2\boldsymbol{r}_{Fo}$$

- If we know I_0 we can calculate what intensity I we would observe (Forward problem – straight forward integration).

- Usually we observe I and would like to know what the original distribution I_0 looks like (Inverse problem – much harder to solve).

Image deblurring: A practical example

Tomography: General ray paths

Tomography aims to derive the distribution of a parameter in the interior of a domain Ω from observations of a diagnostic wave field on the boundary $\partial\Omega$.

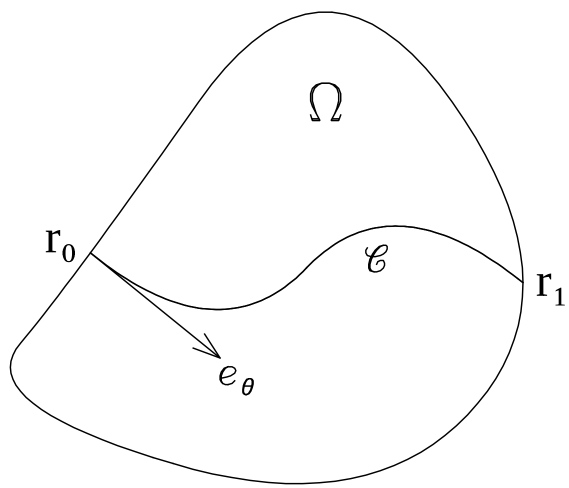

Diagnostic ray path $\mathcal{C}$ through domain Ω from $\boldsymbol{r}_0$ to $\boldsymbol{r}_1$

If, e.g., the refractive index is known, the ray path $\mathcal{C}$ from any $\boldsymbol{r}_0$ to $\boldsymbol{r}_1$ can be calculated and the attenuated intensity

$$I_1(\boldsymbol{r}_0, \boldsymbol{r}_1) = I_0 \exp\left[- \int_{\mathcal{C}(\boldsymbol{r}_0,\boldsymbol{r}_1)\cap\Omega} \kappa(\boldsymbol{r})\, d\boldsymbol{r} \right]$$

can be measured. Deducing the local absorption $\kappa(\boldsymbol{r})$ from these measurements is an inverse problem – a hard one depending on the ray paths $\mathcal{C}$.

Tomography: The X-ray transform

Choose the diagnostic wave so that refractive index is close to unity and κ moderate. So rays are straight along their initial direction $\boldsymbol{e}_\theta$

$$\mathcal{C} = \{\boldsymbol{r}_0 + s\boldsymbol{e}_\theta \mid s \in \mathbb{R}\}$$

Let $s = s_0$ and s_1 be the intersections of $\mathcal{C}$ with $\partial\Omega$, then

$$\underbrace{\ln\left(\frac{I_0 - I_1(\boldsymbol{r}_0,\theta)}{I_0}\right)}_{\text{data}} = \int_{s_0}^{s_1} \kappa(\boldsymbol{r}_0 + s\boldsymbol{e}_\theta)\, ds = \int_\Omega K_\theta(\boldsymbol{r}_0)\underbrace{\kappa(\boldsymbol{r})}_{\text{model}}\, d^3\boldsymbol{r}$$

$$\text{kernel:} \quad K_\theta(\boldsymbol{r}_0) = \int_{s_0}^{s_1} \delta(\boldsymbol{r}_0 + s\boldsymbol{e}_\theta - \boldsymbol{r})\, ds$$

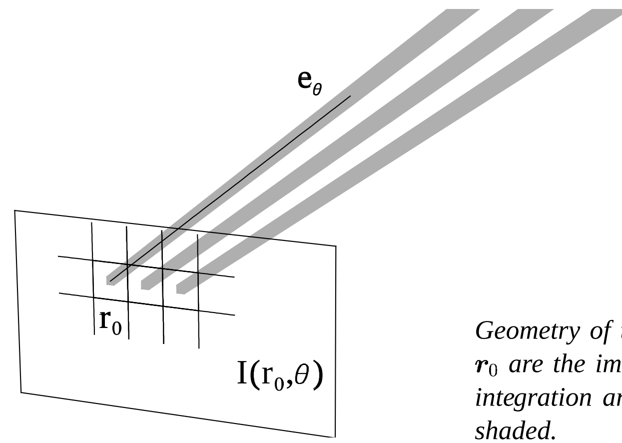

Geometry of the X-ray transform. $\boldsymbol{r}_0$ are the image pixel center, the integration areas (rays) are grey-shaded.

- To investigate a 3D body, take a 2D manifold of positions $\boldsymbol{r}_0$ (image) with a 1D manifold of directions (the scan directions θ should cover $[0, \pi]$)
- If the $\boldsymbol{e}_\theta$ all lie in a plane the 3D X-ray transform decomposes into a set of 2D transforms which can all be solved independently.

Tomography: The Radon transform

We are measuring the line emission from an optically thin plasma cloud with distribution function $f(\boldsymbol{v})$ from different directions $\boldsymbol{e}_\theta$.

The intensity I at frequency ν offset from the line center by $\Delta\nu = \nu - \nu_0$ is proportional to the number of particles which have a velocity component $v = c\Delta\nu/\nu_0$ in direction $\boldsymbol{e}_\theta$.

$$\underbrace{I(\Delta\nu,\theta)}_{\text{data}} = \frac{\int I\,d\nu}{N} \int_{\boldsymbol{v}\cdot\boldsymbol{e}_\theta = c\frac{\Delta\nu}{\nu_0}} \underbrace{f(\boldsymbol{v})}_{\text{model}}\, d^2\boldsymbol{v}$$

where $N = \int f\, d^3\boldsymbol{v}$ (total number of emitting particles) and $\int I\, d\nu$ is independent of direction $\boldsymbol{e}_\theta$ it is measured in, c is the speed of light.

Geometry of the Radon transform. The integration is over planes normal to $\boldsymbol{e}_\theta$ in velocity space.

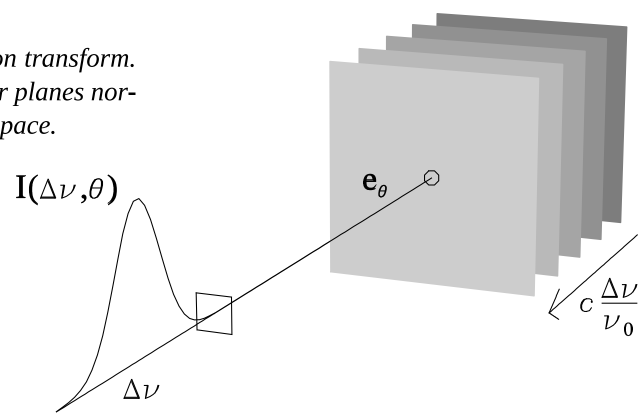

- To get the full 3D distribution measure a 1D manifold of Doppler-shifts $\Delta\nu$ (spectra) in a 2D manifold of directions (the scan directions θ should cover a half sphere).
- In 2D, the X-ray and the Radon transform are actually indentical except that $\boldsymbol{e}_\theta$ is rotated by $\pi/2$.

Radiative transfer: The transport equation

In many atmospheric problems the radiance I_ν at a frequency ν depends only on height z and propagation angle θ.

The radiance $I(z,\theta)$ propagating at an angle θ with respect to the vertical $\hat{\boldsymbol{z}}$ is modified locally by absorption and thermal emission

$$\cos\theta \frac{d}{dz} I_\nu(z,\theta) = -\underbrace{\kappa_\nu(z) I_\nu(z,\theta)}_{\text{absorption}} + \underbrace{\epsilon_\nu}_{\text{thermal emission}} \quad \text{(no scattering)}$$

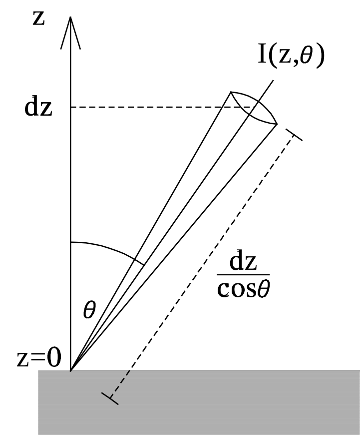

Geometry for the derivation of the radiative transport equation.

Another common approximation is local thermodynamic equilibrium

$$\epsilon_\nu = \kappa_\nu(z) B_\nu(T(z)) \quad \text{where}$$

$$B_\nu(T(z)) = \frac{2h\nu^3}{c^2} \frac{1}{\exp(\frac{h\nu}{k_B T(z)}) - 1}$$

is Planck's function at the local temperature.

Radiative transfer: Up/downward radiances

The integration is simplified by introducing the frequency dependent optical depth

$$\tau_\nu(z) = \int_z^\infty \kappa_\nu(z')\,dz' \quad \text{hence} \quad \kappa_\nu\,dz = -d\tau_\nu$$

The optical thicknes of the entire atmosphere is $\tau_\nu(z=0) \equiv \tau_\nu^{\mathrm{atm}}$.

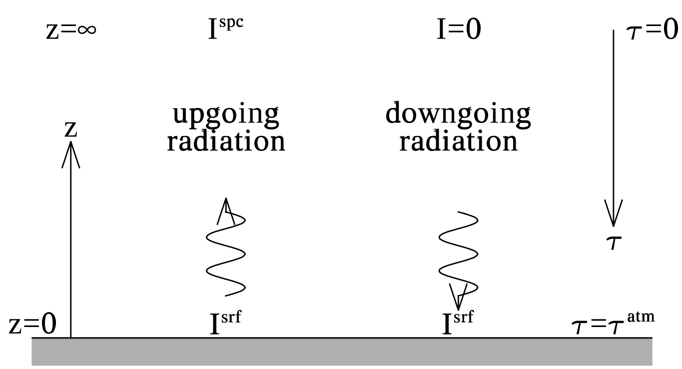

Up/downward radiance boundary values.

Integration for upward propagation ($\cos\theta > 0$) gives the radiance we may observe in space

$$I_\nu^{\mathrm{spc}} = I_\nu^{\mathrm{srf}}\,\mathrm{e}^{-\tau_\nu^{\mathrm{atm}}/\cos\theta} + \int_0^{\tau_\nu^{\mathrm{atm}}} B_\nu(T(\tau_\nu))\,\mathrm{e}^{-\tau_\nu/\cos\theta}\,\frac{d\tau_\nu}{\cos\theta}$$

Integration for downgoing radiation ($\cos\theta < 0$) yields the radiance we observe on the ground when looking upwards

$$I_\nu^{\mathrm{srf}} = \int_0^{\tau_\nu^{\mathrm{atm}}} B_\nu(T(\tau_\nu))\,\mathrm{e}^{-(\tau_\nu^{\mathrm{atm}}-\tau_\nu)/|\cos\theta|}\,\frac{d\tau_\nu}{|\cos\theta|}$$

Radiative transfer: Solar limb darkening equation

The radiance from the Sun for optical ν depends on θ, or, equivalently, on the relative distance $\sqrt{1-\cos^2\theta}$ from the Sun's center

$$\underbrace{I_\nu(\cos\theta)}_{\text{data}} = \frac{1}{\cos\theta}\int_0^\infty \underbrace{\mathrm{e}^{-\tau_\nu/\cos\theta}}_{\text{kernel}}\,\underbrace{B_\nu(T(\tau_\nu))}_{\text{model}}\,d\tau_\nu$$

This equation can be used to infer $B_\nu(T(\tau_\nu))$, hence $T(\tau_\nu)$ from measurment of $I_\nu(\cos\theta)$.

- limb darkening $\Rightarrow$ increase of T with τ_ν
- Kernel $\exp -\tau_\nu/\cos\theta$ is smooth and sensitive only where it varies with $\cos\theta$, i.e., for $\tau_\nu \simeq 0.1\ \ldots\ 1.5$ (lower chromosphere).

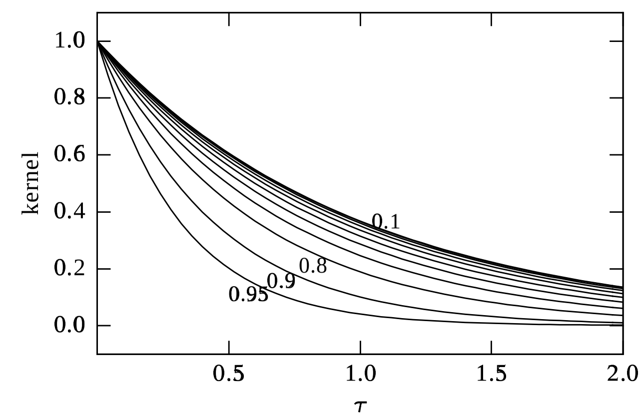

Kernel of the limb darkening equation for $\rho = \sqrt{1-\cos\theta}$ = 0.1, 0.2,…, 0.8, 0.9, 0.95. The solution of the inversion problem $B_\nu(T(\tau_\nu))$ is drawn dashed.

Radiative transfer: Solar limb darkening observations

Observed limb darkening on the Sun – the solar disk.

Observed limb darkening on the Sun – intensity vs. $\mu = \cos\theta$ *for different wavelengths from (Stix, 1989).*

Radiative transfer: Molecular absorption

At GHz and THz frequencies we observe in zenith direction if we assume optically thin conditions ($\tau_\nu \ll 1$) and neglect the galactic background

$$I_\nu = \int_0^\infty B_\nu(T(z))\,\kappa_\nu(z)\,dz$$

For a line at center frequency $\nu_{nm} = (E_m - E_n)/h$ for a transition from state $n \to m$ of a molecule X

$$\kappa_\nu \propto \underbrace{n_{X,n}}_{\substack{\text{density of}\\ \text{X in state } n}} \quad \nu\,\underbrace{\Psi(\nu-\nu_{nm})}_{\text{line shape}} \quad \underbrace{(1-\mathrm{e}^{-\frac{E_m-E_n}{k_BT}})}_{\text{induced emission}}$$

- The density $n_{X,n}$ is related to the concentration c_X

$$n_{X,n} = n_{\text{air}}\,c_X\,\frac{g_n \mathrm{e}^{-\frac{E_n}{k_BT}}}{Z(T)}$$

with g_n the degeneracy of state n and $Z(T)$ is the partition function.

- The line shape collision dominated and well modelled by a Lorentzian line profile

$$\Psi(\nu-\nu_{nm}) = \frac{\Delta\nu_C}{(\nu-\nu_{nm})^2 + (\Delta\nu_C)^2}$$

with width

$$\Delta\nu_C \simeq \Delta\nu_0 \frac{p}{p_0}$$

Radiative transfer: Trace gas inversion

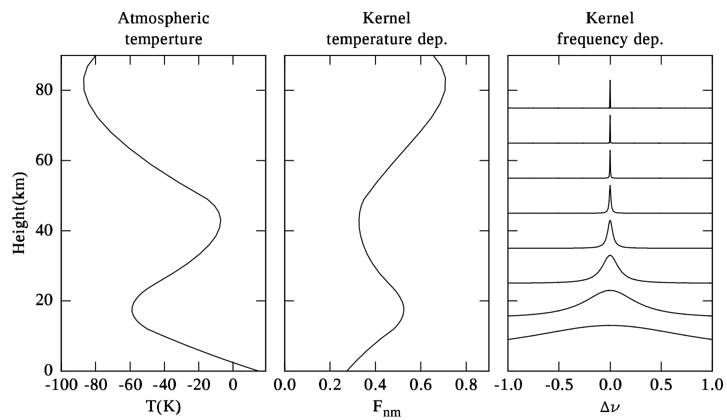

Typical temperature profile of the Earth's atmosphere, factor $F_{n,m}$ and line shape of kernel at various heights.

Insertion yields the inversion problem

$$\underbrace{I_\nu}_{\text{data}} = \int_0^\infty \underbrace{F_{nm}(T(z))}_{\text{model 1}} \underbrace{\frac{\left(\frac{p(z)}{p_0}\right)^2}{\left(\frac{\nu-\nu_{nm}}{\Delta\nu_0}\right)^2 + \left(\frac{p(z)}{p_0}\right)^2}}_{\text{kernel}} \underbrace{c_X(z)}_{\text{model 2}} \, dz$$

where the T dependence is concentrated in

$$F_{nm}(T) \propto B_{\nu_{nm}}(T) \, \frac{E_m - E_n}{k_B T} \, \frac{\mathrm{e}^{-\frac{E_n}{k_B T}} - \mathrm{e}^{-\frac{E_m}{k_B T}}}{Z(T)}$$

- X = CO_2 or O are well mixed so that c_X = const
$\longrightarrow$ solve for $F_{nm}(T(z))$, i.e. $T(z)$.

- If $T(z)$ is known, solve for $c_X(z)$ of more exotic trace gases.

Radiative transfer: Trace gas inversion kernel

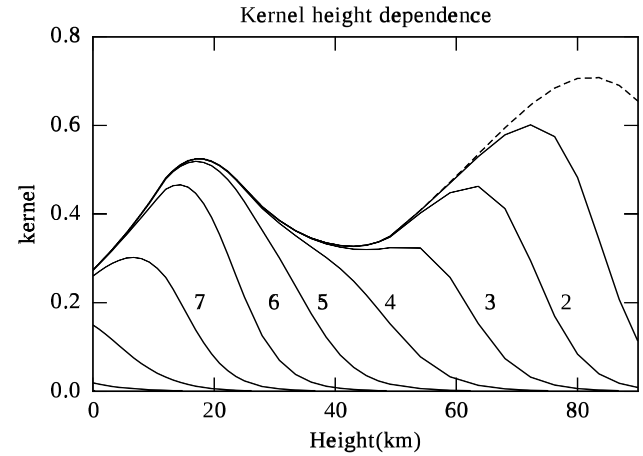

Height dependence of kernel functions with increasing frequency off-set.

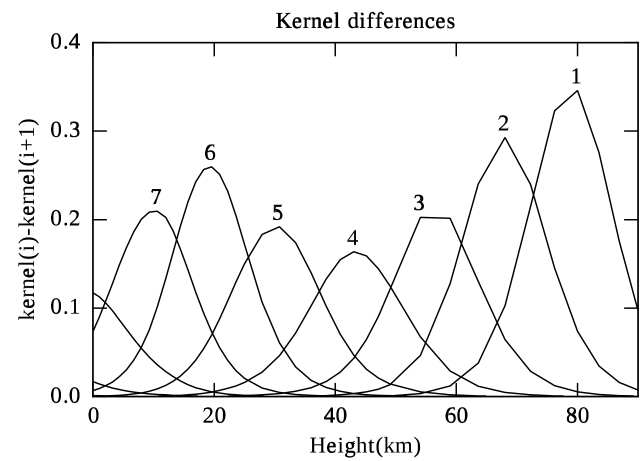

Height dependence of difference between neighbouring kernel functions.

- Combinations of the inversion equation for different $\nu - \nu_{nm}$ may give better kernels.

Helioseismology: Fundamental properties

We assume hydrostatic equilibrium

$$\nabla p_0 = \boldsymbol{g}\rho_0 \quad \text{and} \quad \nabla\cdot\boldsymbol{g} = -4\pi G\rho_0$$

where in our notation $g = \hat{\boldsymbol{r}}\cdot\boldsymbol{g}$ is negative.

The propagation of waves in the Sun is controlled by three further parameters

$$\text{Acoustic speed:} \quad c_s^2 = \frac{\gamma p_0}{\rho_0}$$

$$\text{Brunt-Vaisälä frequency:} \quad N^2 = |g|\left(\frac{\partial_r p_0}{\gamma p_0} - \frac{\partial_r \rho_0}{\rho_0}\right)$$

$$= \frac{|g|}{\gamma}\left(\frac{p_0}{\rho_0^\gamma}\right)^{-1}\frac{\partial}{\partial r}\left(\frac{p_0}{\rho_0^\gamma}\right)$$

$$\text{atmospheric scale height} \quad H = \frac{p_0}{|g|\rho_0} = \frac{c_s^2}{\gamma|g|}$$

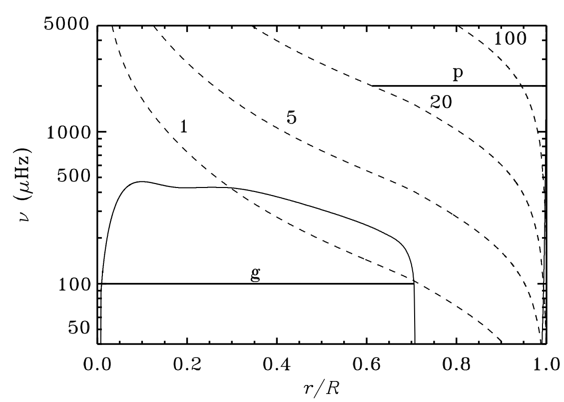

Variation of N (solid) and $c_s k_h$ (dashed) with distance from the center of the Sun for $k_h \simeq \sqrt{l(l+1)}/r$ (Christensen-Daalsgaard, 1998).

Helioseismology: Lagrangian perturbations

The inversion equation is derived from a variaional principle which involves the integration of perturbations over the whole solar volume.

$\longrightarrow$ it is advantageous to change from Eulerian variables

$$\frac{d}{dt}\boldsymbol{v} = -\frac{1}{\rho}\nabla p + \boldsymbol{g}$$

$$\frac{d}{dt}\rho = -\rho\nabla\cdot\boldsymbol{v} \quad \text{and} \quad \frac{d}{dt}p = -\gamma p\nabla\cdot\boldsymbol{v}$$

to Lagrangian variables:

$$\ddot{\boldsymbol{\xi}} = (\gamma-1)\boldsymbol{g}(\nabla\cdot\boldsymbol{\xi}) + c_s^2\nabla(\nabla\cdot\boldsymbol{\xi}) + \nabla(\boldsymbol{g}\cdot\boldsymbol{\xi}) \equiv -\mathcal{A}(\boldsymbol{\xi})$$

$$\delta_L\rho = -\rho_0\,(\nabla\cdot\boldsymbol{\xi}) \quad \text{and} \quad \delta_L p = -\gamma p_0\,(\nabla\cdot\boldsymbol{\xi})$$

On the Sun's surface: $p_0 = \delta_L p = 0$

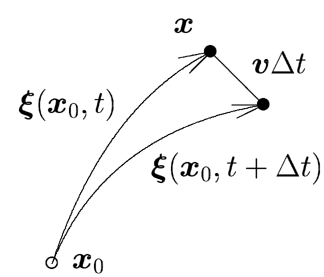

Relation between Eulerian and Lagrangian perturbations for fixed t:

$$\boldsymbol{x} = \boldsymbol{x}_0 + \boldsymbol{\xi}(\boldsymbol{x}_0, t)$$

$$\boldsymbol{v}(\boldsymbol{x}, t) = \dot{\boldsymbol{\xi}}(\boldsymbol{x}_0, t)$$

- The velocity perturbations on the Sun's surface $\dot{\boldsymbol{\xi}}$ can be observed. Usually their FT are considered (for plane parallel geometry):

$$\boldsymbol{\xi}(\boldsymbol{x}_0, t) = \sum_{\boldsymbol{k}_h,\omega} \boldsymbol{\xi}_{\boldsymbol{k}_h,\omega}(z_0)\, e^{i(\boldsymbol{k}_h\boldsymbol{x}_0 - \omega t)} + c.c.$$

Helioseismology: Short wavelength approximation

To qualitatively understand the observations we simplify:

- plane parallel geometry ($r \longrightarrow z$)
- no gravity waves (g-modes are yet undetected)

For $Hk_z \gg 1$ the Lagrangian momentum equation yields

$$\mathrm{div}\ddot{\boldsymbol{\xi}} - c_s^2 \Delta \mathrm{div}\boldsymbol{\xi} \simeq 0$$

For an observed mode with horizontal wavenumber k_h and frequency ω fixed

$$k_z(z)^2 \simeq \frac{\omega^2}{c_s^2(z)} - k_h^2$$

Since c_s increases with depth we have reflection between the surface $z = 0$ and some z_{rfl} inside the Sun.

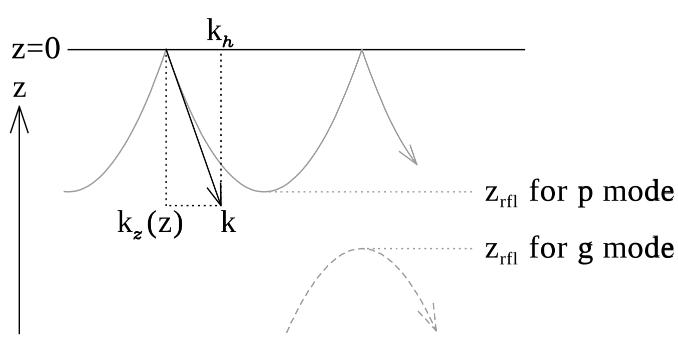

Propagation paths of an acoustic wave (p-mode) in the Sun. In comparison, the propagation of gravity waves (g-mode) is dashed.

- In between the reflection points, the wave must have an integer number of nodes

$$\int_{z_{\mathrm{rfl}}}^{0} k_z(z)\, dz = (n + \alpha_{\mathrm{rfl}} + \alpha_0)\pi$$

where $\alpha_{0,\mathrm{rfl}}$ are phase corrections at the respective reflection height (from observations: $\alpha_{\mathrm{rfl}} + \alpha_0 \simeq 1.45$)

Helioseismology: Short wavelength dispersion

With $N^2 \simeq 0$, we can roughly estimate how c_s increases with depth inside the convection zone:

$$\frac{1}{c_s^2}\frac{dc_s^2}{dz} = \left(\frac{1}{p_0}\frac{dp_0}{dz} - \frac{1}{\rho_0}\frac{d\rho_0}{dz}\right)$$
$$= \left(\frac{1}{p_0}\frac{dp_0}{dz} - \frac{1}{\gamma p_0}\frac{dp_0}{dz}\right) = (1-\frac{1}{\gamma})\frac{g\rho_0}{p_0} = (\gamma-1)\frac{g}{c_s^2}$$

Insert $c_s^2(z)$ into the equation for $k_z^2(z)$

$$k_z^2(z) \simeq \frac{\omega^2}{(\gamma-1)gz} - k_h^2$$

Insertion of $k_z(z)$ into node number integral gives

$$\int_{z_{\mathrm{rfl}}}^{0} \sqrt{\frac{\omega^2}{(\gamma-1)gz} - k_h^2}\;\, dz = k_h |z_{\mathrm{rfl}}| \frac{\pi}{2} = (n + \alpha_{\mathrm{rfl}} + \alpha_0)\pi$$

where $z_{\mathrm{rfl}} = (\omega/k_h)^2/(\gamma-1)g$. The last equation yields the observable relation between the frequency and horizontal wavenumber

$$\omega^2 = \omega^2_{\boldsymbol{k}_h,n} \simeq 2(\gamma-1)g\,(n + \alpha_{\mathrm{rfl}} + \alpha_0)k_h$$

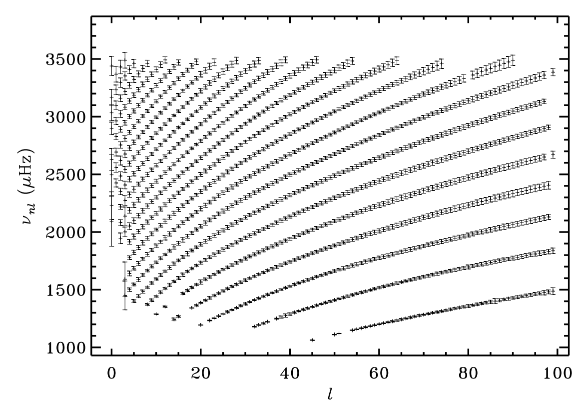

Observed dispersion for acoustic modes inside the Sun with $l \simeq k_h R_\odot$

Helioseismology: The variational principle

Introduction of the Fourier transform in the Lagrangian momentum equation gives

$$\omega^2_{\boldsymbol{k}_h,n}\boldsymbol{\xi}_{\boldsymbol{k}_h,n} = \mathcal{A}_{\boldsymbol{k}_h}(\boldsymbol{\xi}_{\boldsymbol{k}_h,n}) \qquad (1)$$

an eigenvalue problem for eigenvalues $\omega^2_{\boldsymbol{k}_h,n}$ and eigenstates $\boldsymbol{\xi}_{\boldsymbol{k}_h,n}$.

Since $\mathcal{A}_{\boldsymbol{k}_h}$ is hermitian, the eigenstates span a Hilbert space with normalization

$$\int_{-\infty}^{0} \rho_0 \left(\boldsymbol{\xi}^*_{\boldsymbol{k}_h,m}(z)\cdot\boldsymbol{\xi}_{\boldsymbol{k}_h,n}(z)\right)\, dz = \delta_{m,n} M_{\boldsymbol{k}_h,n} \quad \text{(mode inertia)} \qquad (2)$$

hence the above eigenvalue equation (1) can also be written as

$$\omega^2_{\boldsymbol{k}_h,n} M_{\boldsymbol{k}_h,n} = \int_{-\infty}^{0} \rho_0 \left(\boldsymbol{\xi}^*_{\boldsymbol{k}_h,n}\cdot\mathcal{A}_{\boldsymbol{k}_h}(\boldsymbol{\xi}_{\boldsymbol{k}_h,n})\right)\, dz \qquad (3)$$

• If the calculated $\omega^2_{\boldsymbol{k}_h,n}$ do not agree with the observed frequencies, we have to vary ρ_0 (and all other parameters accordingly) in our model:

$$\rho_0 \to \rho_0 + \delta\rho_0 \quad \text{causes} \quad p_0 \to p_0 + \delta p_0 \quad ; \quad g \to g + \delta g$$
$$\mathcal{A}_{\boldsymbol{k}_h} \to \mathcal{A}_{\boldsymbol{k}_h} + \delta\mathcal{A}_{\boldsymbol{k}_h} \quad ; \quad \boldsymbol{\xi}_{\boldsymbol{k}_h,n} \to \boldsymbol{\xi}_{\boldsymbol{k}_h,n} + \delta\boldsymbol{\xi}_{\boldsymbol{k}_h,n}$$
$$\text{and finally} \quad \omega^2_{\boldsymbol{k}_h,n} \to \omega^2_{\boldsymbol{k}_h,n} + \delta(\omega^2_{\boldsymbol{k}_h,n})$$

We may vary the eigenvalue equation (1) but then we need the perturbations of the eigenstates as well. A more convenient approach is to vary (3). The procedure then is almost identical to conventional perturbation theory in quantum mechanics. In any case, the orthogonality (2) and the mode inertia $M_{\boldsymbol{k}_h,n}$ remain invariant under the variation.

Helioseismology: The inversion problem

The variation of (3) yields

$$\delta(\omega^2_{\boldsymbol{k}_h,n}) M_{\boldsymbol{k}_h,n} = \int_{-\infty}^{0} \rho_0 \left(\boldsymbol{\xi}^*_{\boldsymbol{k}_h,n}\cdot\delta\mathcal{A}_{\boldsymbol{k}_h}(\boldsymbol{\xi}_{\boldsymbol{k}_h,n})\right)\, dz$$

Hence the variation of the eigenvalue is obtained from the variation of the operator $\mathcal{A}_{\boldsymbol{k}_h}$ with respect to the unperturbed eigenfunctions. The perturbed eigenfunctions are not required.

Next, relate the variation $\delta\mathcal{A}_{\boldsymbol{k}_h}$ to the appropriate variation $\delta\rho_0$ (Fréchet derivative $\propto \mathcal{K}_{\boldsymbol{k}_k}$). We finally obtain after renormalization:

$$\underbrace{\frac{\delta(\omega^2_{\boldsymbol{k}_h,n})}{\omega^2_{\boldsymbol{k}_h,n}}}_{\text{data}} = \int_{-\infty}^{0} \underbrace{\mathcal{K}_{\boldsymbol{k}_h}(\boldsymbol{\xi}^*_{\boldsymbol{k}_h,n}, \boldsymbol{\xi}_{\boldsymbol{k}_h,n})}_{\text{kernel}} \underbrace{\frac{\delta\rho_0}{\rho_0}}_{\text{model}}\, dz$$

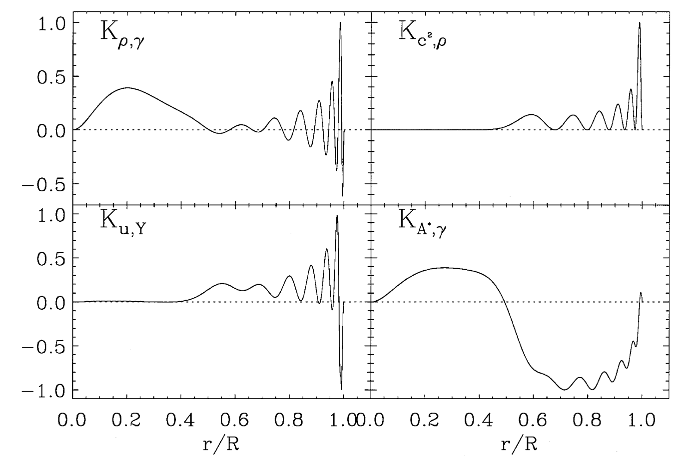

Kernel functions $K_{\boldsymbol{k}_h}$ for an acoustic mode $k_h \simeq \sqrt{l(l+1)}/R_\odot$ with l = 10 and eigenfunction order n = 6. The first subscript parameter is varied, the second fixed. Here, $u = c_s^2/\gamma$, $A^* \propto N^2/|g|$ and $Y \propto$ He abundance (Kosovichev, 1999).